The 2009 IEEE/RSJ International Conference on
Intelligent Robots and Systems
October 11-15, 2009 St. Louis, USA

Motion planner and lateral-longitudinal controllers for autonomous maneuvers of a farm vehicle in headland

Christophe Cariou*, Roland Lenain*, Benoit Thuilot†, Philippe Martinet†
* Cemagref
24, av. des Landais
63172 Aubière Cedex France
christophe.cariou@cemagref.fr
† LASMEA
24, av. des Landais
63177 Aubière Cedex France
benoit.thuilot@lasmea.univ-bpclermont.fr

***Abstract*— This paper addresses the problem of path generation and motion control for the autonomous maneuvers of a farm vehicle in headland. A reverse turn planner is firstly investigated, based on primitives connected together to easily generate the reference motion. Then, both steering and speed control algorithms are presented to accurately guide the vehicle. They are based on a kinematic model extended with additional sliding parameters and on model predictive control approaches. Real world experiments have been carried out on a low adherent terrain with an experimental mobile robot. At the end of each row, the reverse turn is automatically generated to connect the next reference track, and the maneuver is autonomously performed by the vehicle. Reported experiments demonstrate the capabilities of the proposed algorithms.**

I. INTRODUCTION

With a world population exceeding 6 billion and growing by about 6 million a month, the need to increase agricultural production while reducing the negative impacts of farm activity on the environment has become critical. Although modern agriculture allowed to double the world food production in 35 years, intensive use of inputs (chemical fertilizers, pesticides, herbicides) and increasingly size of farm vehicles are currently questioned due to their major degrading effects on the aquatic and terrestrial ecosystems. Therefore, new solutions are today required to develop environmentally sustainable agricultural productions. In this framework, as pointed out in [4] and [9], precision agriculture together with the development of automatic guided vehicles constitutes a promising way in terms of accuracy, repeatability, durability and field efficiency.

Numerous auto-steering systems have already been proposed and marketed for semi-autonomous tractors to accurately follow parallel tracks in the field (*e.g. Agco autoguide, Agrocom e-drive, Autofarm autosteer, John-Deere autotrac, Trimble aggps, Reichhardt autosteer*). However, the driver has still to manually turn the vehicle at the end of each row. In order to benefit of fully automated solutions, the automation of maneuvers in headlands is required. Very few approaches have been proposed in that way, moreover mainly based on loop turns (*e.g. John-Deere itecpro*), [15]. The drawback of such an approach is that it involves excessive headland width for turning on the adjacent track, and is thereby far from optimal in term of productivity, headland being usually low-yield field areas due to high soil compaction. A more efficient solution is to perform reverse turns, i.e. maneuvers executed with stop points and reverse motion, leading to reduced headlands as highlighted on figure 1. This type of maneuver is widely used by farmers and more in accordance with agricultural European practices.

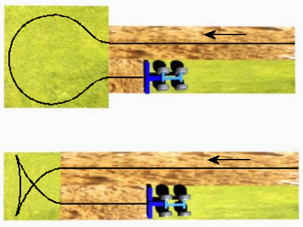

Fig. 1. Loop turn and reverse turn

However, automation of such a maneuver is a challenging problem in both path planning and control point of views. In particular, as pointed out in [14], wheel skidding and sliding are inevitable in an agricultural context and may seriously damage the accuracy of path tracking. Delays induced by steering and speed actuators may also lead to transient lateral overshoots when the vehicle enters into curves, or longitudinal overshoots when it stops.

In the literature, numerous researches have mainly focused on planning the global trajectories in the whole field to increase field efficiency [2], and very few works relate maneuvers generation and vehicle control in headlands [12]. Moreover, most wheeled mobile robot controllers have been developed without sliding and actuator delays accounted, and consider most often the speed as constant.

This paper proposes to address this issue and is organized as follows. First, a trajectory generation strategy is presented based on primitives connected together with the aim to easily generate reverse turns. Next, the steering controller is considered. As in our previous work on path following for two [6] and four [3] wheel steering vehicles, the steering controller is based on a kinematic model extended with sliding parameters to take into account for sliding phenomena. A predictive action is also added to reduce the effects induced by both steering actuation delays and machine inertia. Next, the velocity controller is designed based on a model predictive control approach in order to anticipate for vehicle speed variations. Finally, the capabilities of the proposed algorithms are insvestigated through full-scale experiments.

II. Reverse turn motion planner

The planning of a reverse turn in a free obstacle headland consists in generating three successive motions $\{M1, M2, M3\}$, see figure 2, to connect two adjacent tracks AB and CD separated from a distance d, while obeying vehicle's kinematic and dynamic constraints and minimizing some criteria, e.g. path length, headland size, time spent or control effort.

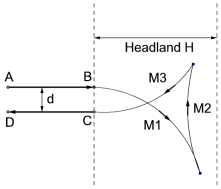

Fig. 2. Three motions in a reverse turn

In the literature, such a problem is mainly addressed using generic optimal control algorithms, designed to find optimal point-to-point trajectories for a given cost function from a wide variety of configurations, see [8], [12]. These approaches are based on kino-dynamic models to produce smooth trajectories and demand high computational cost, so that they can hardly be used on-line.

In this section, we propose an alternative method using elementary primitives (line segment, arc of circle) connected together with usual pieces of clothoid to ensure curvature continuity, see [7], [11]. Such primitives-based planning approaches are widely used in the literature using either clothoids, polynomial splines, cubic spirals or elasticas to construct non-holonomic motion. The proposed approach is well-suited to the reverse turn, and allows to rapidly obtain an efficient path planning solution to test control algorithms.

A. Definition of an arc of clothoid admissible for the vehicle

The aim of this subsection is to define an arc of clothoid BP_1, see figure 4(a), feasible for the considered two-front steering vehicle presented on figure 3, in order to connect a line segment AB to a circle of radius R corresponding to the minimum curvature radius of the vehicle.

- Max. front-wheel steering angle $\delta_{Fm} = 25°$
- Max. front-wheel steering rate $\omega_a = 20°/s$
- Ref. vehicle linear velocity $v_{ref} = 1.75m/s$
- Max. longitudinal acceleration $a_m = 1m/s^2$
- Wheel base $L = 1.2m$
- Wheel track $V = 1.0m$

Fig. 3. Experimental vehicle and its main parameters

The curvature c of a clothoid varies linearly with respect to its curvilinear abscissa s, see generic equation (1) and corresponding shape illustrated on figure 4(a).

$$c = g.s \tag{1}$$

Using (1) and the following geometric relation

$$c_V = \frac{tan\delta_F}{L} \tag{2}$$

where c_V denotes the vehicle curvature, it can be deduced that (perfect tracking has been assumed, so that $c = c_V$)

$$g = \frac{dc}{ds} = \frac{dc_V}{ds} = \frac{1}{L\cos^2\delta_F}.\frac{d\delta_F}{ds} \tag{3}$$

Then, for the considered vehicle, a suitable proportionality coefficient g can be computed: in view of the maximum steering rate of the wheels ω_a and of the reference vehicle linear velocity v_{ref} during the reverse turn, we have $\frac{d\delta_F}{ds} = 0.11°/cm$. Reporting this value into (3) supplies the relation $g = f(\delta_F)$ depicted on figure 4(b). g is finally chosen as $g_{min} = 0.166$ so that the arc of clothoid is admissible by the vehicle whatever δ_F. To avoid saturation of the steering actuator, this value will be reduced of 10% in the following, i.e. $g = 0.15$. For the same reason, R is chosen as $\frac{L}{tan(20°)} = 3.29m$. Obviously, as presented on figure 4(a), only the arc of clothoid BP_1 will be performed by the vehicle until the circle of radius R is reached at P_1, corresponding to the curvilinear abscissa $s_1 = \frac{1}{g.R} = 2.02m$.

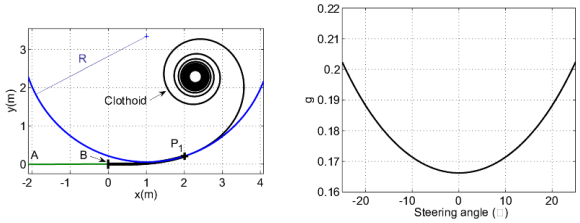

(a) Clothoid, $g = 0.15$ (b) $g = f(\delta_F)$

Fig. 4. Clothoid and computation of g

As detailed in [13] for highway design, the Cartesian coordinates of the clothoid can be written using Fresnel integrals, which can be approximated using different methods, e.g. trapezoids method or development in Taylor series. The arc of clothoid BP_1 can thus be entirely defined to connect the line segment to the circle of radius R, leading to continuous curvature trajectories admissible for the vehicle.

B. Trajectory generation strategy

The easiest approach consists in generating a fish-tail maneuver, usually performed by self-propelled vehicle or tractor with mounted implement. It is composed of two arcs of clothoid ($Cl1$, $Cl2$) from points B and C and three arcs of circle, as depicted on figure 5. At stop points S_1 and S_2 (the tangency points at circles of radius R), the direction of the wheels will be reorientated to change the vehicle rotation instantaneous center from I_1 to I_2 and from I_2 to I_3.

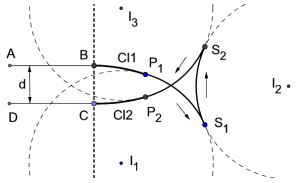

Fig. 5. Fish-tail maneuver

Figures 6(a) and 6(b) present the results for respectively $d = 0m$ and $d = -2m$, the vehicle body being represented

by a rectangle of size L (wheel base) $\times$ V (wheel track). The headland width stays around $h = 5m$, with a total path length $l = 12m$ in both case. For comparison, a loop turn with $d = 0m$ as presented on figure 7 will require twice more headland width ($11m$) and twice more path length ($26m$).

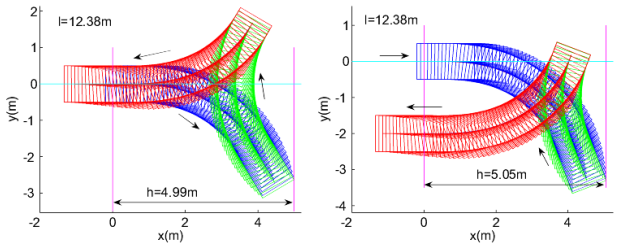

(a) $d = 0m$ (b) $d = -2m$

Fig. 6. Fish-tail maneuver

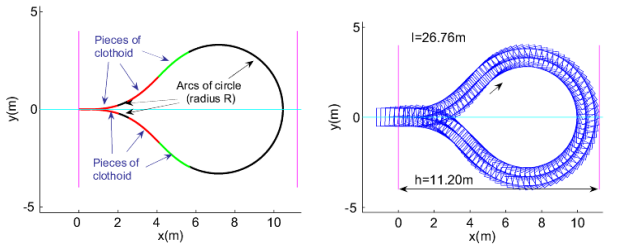

(a) Construction $d = 0m$ (b) Result

Fig. 7. Loop turn, $d = 0m$

Other motions could be defined, reducing slighty the width of the headland, pointing out that the simple fish-tail maneuver is not optimal with respect to the headland size. In the case presented on figure 8(a), the third motion is firstly calculated so that the vehicle is parallel to the headland limit. The headland width is $h = 4m86$, i.e. a reduction about $13cm$ as regard to the fish-tail approach. The origin of this slight difference is shown on figure 8(b). However, this solution requires an excessive long path length ($23m$).

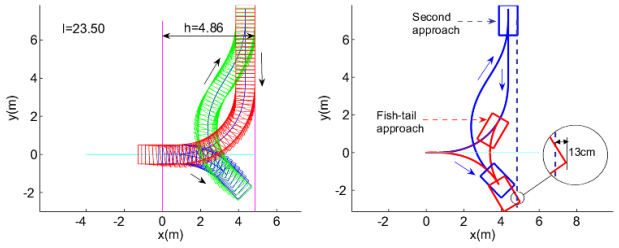

(a) d=0m (b) Comparison

Fig. 8. Second approach

C. Speed reference

At each point of the planned trajectories is associated a speed reference. It is chosen in order to obtain a maximum acceleration that does not exceed 10% of the maximum longitudinal acceleration a_m, i.e $0.9m/s^2$. Figure 9(a) presents a first solution with a constant acceleration $0.9m/s^2$, leading to a small time ($1.9s$) and small distance ($1.7m$) to reach $v_{ref} = 1.75m/s$. However, this solution tested in real conditions on low friction coefficient surfaces (wet grass, muddy ground) leads to important sliding and skidding phenomena. In fact, as the longitudinal acceleration phase takes place during curves, the vehicle undergoes a strong lateral acceleration (centrifugal acceleration) and the rear tires easily lost lateral stability whereas the front wheels present excessive slip to counteract such an oversteer phenomenon. Other solutions, such as those depicted on figure 9(b) based on a sigmoid function, are then preferred in order to obtain smoother accelerations, especially at each beginning/end of motions.

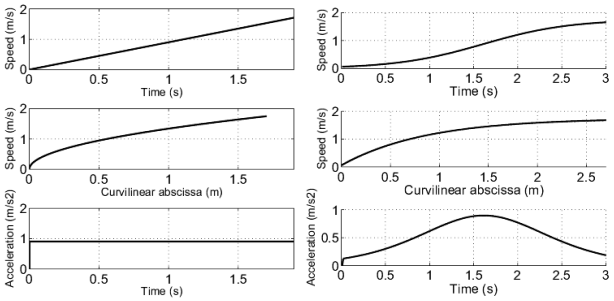

(a) Constant acceleration (b) Speed in sigmoid form

Fig. 9. Speed reference

With the motion planner presented in this section, using geometric primitives connected together and the associated speed reference, the reverse turns can now be easily defined. The next section presents the control algorithms developed to accurately follow such trajectories.

III. Control Algorithms

Accurate automatic guidance of mobile robots in an agricultural environment constitutes a challenging problem, mainly due to the low grip conditions usually met in such a context. As pointed out in [14], if the control algorithms are designed from pure rolling without sliding assumptions, the accuracy of path tracking may be seriously damaged, especially in curves. Therefore, sliding has to be accounted in the control design to preserve the accuracy of path tracking, whatever the path to be followed and soil conditions. Moreover, the actuation delays may lead to significant overshoots, especially at each beginning/end of curves and at each stop points. Predictive actions have therefore to be defined in order to maintain accurate path tracking performances.

Subsection A presents an extended kinematic model accounting for sliding effects and addresses the estimation of grip conditions using an observation algorithm. Subsection B describes the steering and speed control algorithms.

A. Kinematic model extended with sliding parameters

In the same way than in our previous work [6], two parameters homogeneous with sideslip angles in a dynamic model are introduced to extend the classical two-wheel steering kinematic model, see the bicycle representation of the vehicle on figure 10. These two angles denoted respectively β_F and β_R for the front and rear axle represent the difference between the theoretical direction of the linear velocity vector at wheel centers, described by the wheel plane, and their

actual direction. These angles are assumed to be entirely representative of the sliding influence on vehicle dynamics. The notations used in this paper are listed below and depicted on figure 10.

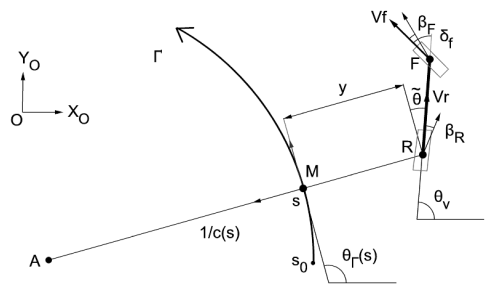

Fig. 10. Path tracking parameters

- F and R are respectively the center of the front and rear virtual wheels. R is the point to be controlled.
- θ_v is the orientation of vehicle centerline with respect to an absolute frame $[O, X_O, Y_O)$.
- δ_F is the front steering angle and constitutes the first control variable.
- V_r is the vehicle linear velocity at point R and constitutes the second control variable.
- β_F and β_R are the front and rear sideslip angles.
- M is the point on the reference path Γ to be followed, which is the closest to R.
- s is the curvilinear abscissa of point M along Γ.
- $c(s)$ is the curvature of the path Γ at point M.
- $\theta_\Gamma(s)$ is the orientation of the tangent to Γ at point M with respect to the absolute frame $[O, X_O, Y_O)$.
- $\tilde{\theta} = \theta_v - \theta_\Gamma$ is the vehicle angular deviation.
- y is the vehicle lateral deviation at point R.

The equations of motion are derived with respect to the path Γ. It can be established, see [6], that:

$$\begin{cases} \dot{s} &= V_r \frac{\cos(\tilde{\theta}-\beta_R)}{1-c(s)\,y} \\ \dot{y} &= V_r \sin(\tilde{\theta}-\beta_R) \\ \dot{\tilde{\theta}} &= V_r \left[\cos(\beta_R)\lambda_1 - \lambda_2\right] \end{cases} \quad (4)$$

with: $\lambda_1 = \frac{\tan(\delta_F-\beta_F)+\tan(\beta_R)}{L}$, $\lambda_2 = \frac{c(s)\cos(\tilde{\theta}-\beta_R)}{1-c(s)\,y}$

Model (4) accurately describes the vehicle motion in presence of sliding as soon as the two additional parameters β_F and β_R are known. An observation algorithm has been developed to achieve sideslip angles indirect estimation, relying on the sole lateral and angular deviations measurements, see [5]. This observer is based on the duality between observation and control, and is studied as a classical control problem. The overall scheme of this observer is presented on figure 11. β_F and β_R are considered as control variables to be designed in order to ensure the convergence of the extended model outputs $(y, \tilde{\theta})_{obs}$, to the measured variables $(y, \tilde{\theta})_{mes}$.

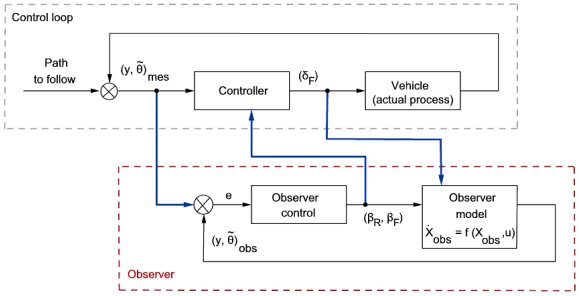

Fig. 11. Observer overall scheme

B. Control laws design

The extended model (4) constitutes a relevant basis for mobile robot control design. The control objective is on one hand to perform an accurate path tracking with respect to lateral and angular deviations, and on the other hand to control the vehicle velocity on the planned speed references.

1) Steering controller: In our previous work [6], model (4) has been turned into chained form and the following steering control law for the front axle (5) has been derived (K_d is a gain allowing to specify a settling distance).

$$\begin{aligned} \delta_F &= \beta_F + \arctan\Big\{ \tan(-\beta_R) \\ &\quad + \frac{L}{\cos(\beta_R)}\Big(\frac{c(s)\cos\tilde{\theta}_2}{\alpha} + \frac{A\cos^3\tilde{\theta}_2}{\alpha^2}\Big)\Big\} \end{aligned} \quad (5)$$

with:

$$\begin{cases} \tilde{\theta}_2 &= \tilde{\theta} - \beta_R \\ \alpha &= 1 - c(s)y \\ A &= -\frac{K_d^2\, y}{4} - K_d\,\alpha\tan\tilde{\theta}_2 + c(s)\alpha\tan^2\tilde{\theta}_2 \end{cases} \quad (6)$$

To reject transient overshoots in lateral deviation when the vehicle enters into a curve, mainly due to delays induced by the steering actuator and vehicle inertia, a predictive action has been added, see [5]. Experimental results have demonstrated that high accurate guidance can be achieved whatever the grip conditions and the shape of the path to be followed. However, the vehicle velocity was manually controlled and strictly positive. The objective in this paper is to extend these results and take advantage that the path following performances were demonstrated to be independent from the vehicle velocity, see [6], to built a second control loop dedicated to speed control, in order that reverse turn can be achieved autonomously.

2) Speed controller: Usually, when a vehicle stops at a point, signifiant overshoots in longitudinal motion are observed, mainly due to engine delay and inertia if they are not accounted in the controller. One way to reject such a problem, and anticipate speed variations, is to design a predictive algorithm. To achieve this objective, Model Predictive Control techniques (see [10]) are here used.

Let us denote $n\,T_e$ the current time instant, with T_e the sampling period *($T_e = 0.1s$ in our case)*. Since the speed reference at each point of the maneuver is known, the desired value $D_{[n+H]}$ for the vehicle velocity after an horizon of prediction $H\,T_e$ ($H = 10$) can be inferred from the current

vehicle position (i.e. at time $n\,T_e$). Then, relying on an actuator model, a control sequence $(C_{[n]}, \ldots, C_{[n+H]})$ to be sent to the actuator is computed, with the aim that the vehicle actual velocity V follows some ideal reference trajectory T tending towards $D_{[n+H]}$. Finally, only the first term of the sequence (i.e. $C_{[n]}$) is actually sent, at time $n\,T_e$. More precisely, T is classically chosen as a first order dynamic (see figure 12):

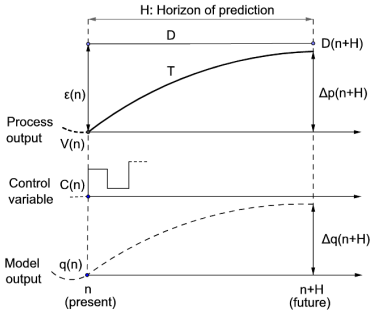

Fig. 12. Model Predictive Control

$$T_{[n+i]} = D_{[n+H]} - \left(D_{[n+H]} - V_{[n]}\right)\lambda^i \;\;, 0 < \lambda < 1 \quad (7)$$

Then, in order to limit computing time, only one coincidence point is here considered to derive the control sequence. This means that a constant control sequence $C_{[n]} = C_{[n+1]} = \ldots = C_{[n+H]}$ is looked for, with the objective that the actuator model output q meets reference trajectory T at time $(n+H)\,T_e$. Since the actuator model has been identified as a first order system, with time constant $\tau = 0.42\ s$ and gain $K = 0.97$, then $q_{[n+H]}$ can be shown to be (just evaluate at $t = H\,T_e$ the celebrated continuous first order step response from initial condition $q_{[n]} = V_{[n]}$):

$$q_{[n+H]} = V_{[n]} e^{-\frac{H\,T_e}{\tau}} + C_{[n]}\,K\left(1 - e^{-\frac{H\,T_e}{\tau}}\right) \quad (8)$$

Therefore, from (7) and (8), it can be deduced that the control value $C_{[n]}$ ensuring $q_{[n+H]} = T_{[n+H]}$ is:

$$C_{[n]} = \frac{\left(D_{[n+H]} - V_{[n]}\right)\left(1 - \lambda^H\right) + V_{[n]}\left(1 - e^{-\frac{H\,T_e}{\tau}}\right)}{K\left(1 - e^{-\frac{H\,T_e}{\tau}}\right)} \quad (9)$$

Equation (9) is the proposed predictive speed controller. Furthermore, to take into account the time delay (rT_e) on the speed actuator ($r = 2$), we can either introduce it in (8) or simply initialize the reference trajectory on $V_{[n+r]}$. Indeed, if the system has a delay r while the model (8) is considered without delay, we have: $V_{[n]} = q_{[n-r]}$, $V_{[n+r]} = q_{[n]}$, thus $V_{[n+r]} = V_{[n]} + q_{[n]} - q_{[n-r]}$, i.e. the prediction of the process at $n + r$, easy to estimate as all the terms are known.

IV. Experimental results

In this section, capabilities of the proposed control algorithms are investigated on an irregular natural terrain composed of mud and wet grass, using the front two-wheel steering experimental mobile robot depicted on figure 3. The only exteroceptive sensor on-boarded is an RTK-GPS receiver, whose antenna has been located straight up the center of the vehicle rear axle. It supplies an absolute position accurate to within 2cm, at a 10Hz sampling frequency.

In our first experiments, the vehicle heading was derived from the velocity measurement supplied by the GPS. However, the main drawback of such an approach is that the accuracy of the heading strongly depends on the vehicle velocity. In fact, at low speed, even after being processed through a Kalman state reconstructor, the obtained heading was quite noisy. Therefore, a gyrometer has been preferred to obtain an accurate heading during the maneuvers.

In the forthcoming experimental tests, the track AB is firstly recorded during a preliminary run achieved in manual driving. The reverse turn at the end of the track is then automatically calculated with $d = -2m$, as well as the trajectory back CD. Finally, the path is autonomously followed by the vehicle using the steering control law from [5] and speed control law (9), see the result figure 13. The lateral deviation according to the curvilinear abscissa is reported on figure 14.

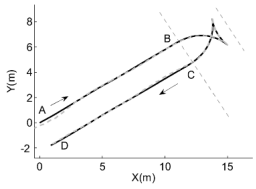

Fig. 13. Result of the path following

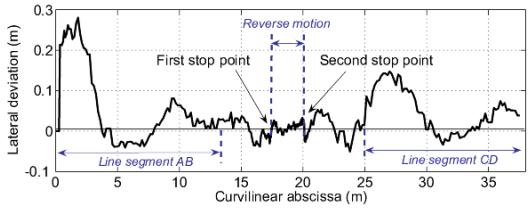

Fig. 14. Lateral deviation

At the beginning, the vehicle starts at about $25cm$ from the path to follow. It reaches then the planned path and maintains (in spite of fast speed and steering variations) an overall lateral error about $\pm 5cm$ until the first stop point. The reverse motion is also satisfactorily carried out, as well as the back motion, except at the end of the curve with a lateral deviation about $15cm$. In fact, the vehicle goes out of the curve at full speed with the front wheels still compensating for the sliding effects during the curve. Although the predictive action reduces significantly overshoots due to actuator delays, the fast variation in the sliding conditions may lead to such overshoots. Therefore, the sideslip angles observer needs to be more reactive. This will demand the integration of dynamic features (center of gravity, moments of inertia, ...) into the observer algorithm, in order to decrease estimation delays and improve accuracy at such transient phase at high speed (to be investigated in future development).

The speed reference according to the curvilinear abscissa is reported on the top of figure 15. The velocity $v_{ref} = 1.75m/s$ is correctly followed. The speed variations are well anticipated with the predictive approach, with accelerations

not exceeding $a_m = 1m/s^2$. On the bottom of figure 15 is also reported the measured and control signals of the front steering angle. We observe that the steering control is quite smooth and that the measured angle of the wheels follows correctly the steering control, remaining inside $\pm 25°$ (maximum front-wheel steering angle). At the stop points, the direction of the wheels is correctly reorientated to change the vehicle instantaneous rotation center.

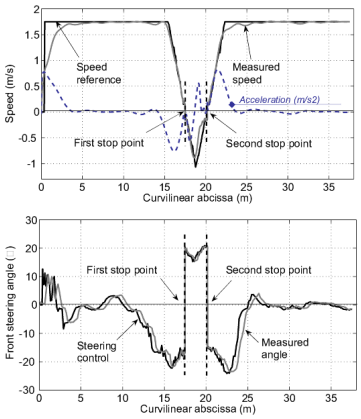

Fig. 15. Speed and steering controls

These results show that planned motions obeying vehicle's kinematic and dynamic constraints together with sliding estimation and lateral/longitudinal controllers with predictive actions, enable to obtain correct path following results for off-road mobile robots, even on maneuvers with stop points.

V. Conclusions and future work

This paper adresses the problem of motion generation and control of autonomous farm vehicles in headlands. A reverse turn path planning algorithm is firstly presented. The trajectories are built using elementary primitives (line segment, arc of circle) connected together with piece of clothoid in order to ensure the curvature continuity of the motions. This simple approach enables to rapidly obtain an efficient path planning solution to test the motion control algorithms. An extended kinematic model accounting for sliding effects via two additional sideslip angles is then presented. This model is used to derive a steering control algorithm independent from the vehicle velocity. A second control loop dedicated to the vehicle speed control is then investigated based on model predictive algorithm to anticipate speed variations and compensate for low-level capabilities.

Promising results are presented with an off-road experimental mobile robot on a fish-tail maneuver. In spite of fast speed and steering variations required to perform such maneuver, an overall tracking error within $\pm 5cm$ is obtained, except on the third motion with a punctual lateral deviation about $15cm$, mainly due the lack of reactivity of the sideslip angles observer. This last point is the object of further development based on the design of mixed kinematic and dynamic observer.

Moreover, this system could be advantageously coupled with a device performing repetitive actions on the vehicle, such as the control of the hitches, the power take-off and the hydraulic valves (see [1]), in order to relieve the human driver of such tasks during headland turns. Furthermore, the execution of maneuvers with a four-wheel steering vehicle is currently also investigated to explicitly control both lateral and angular deviations (see first developments on path following task in [3]). Finally, we also plan to investigate the case of the reverse turn with a trailer connected to the vehicle. Since we are concerned with agricultural applications, such a maneuver with large trailers constitutes another challenging problem, all the more in high sliding and skidding conditions.

References

[1] Berducat M., Devaux J.F., Poirier J.P. *Method and device for automatizing repetitive tasks on a machine* Patent EP0903656, 2003.

[2] Bochtis D.D., Vougioukas S.G. *Minimising the non-working distance travelled by machines operating in a headland field pattern* Biosystems engineering 101:1-12, 2008.

[3] Cariou C., Lenain R., Thuilot B., Martinet P. *Adaptive control of four wheel steering off road mobile robots: application to path tracking and heading control in presence of sliding* IEEE/RSJ Int. conf. on intelligent robots and systems, Nice, France, September 22-26, 2008.

[4] Katupitiya J., Eaton R., Yaqub T. *Systems engineering approach to agricultural automation: new developments* In IEEE Systems Conference, Honolulu, Hawai, USA April 9-12 2007.

[5] Lenain R., Thuilot B., Cariou C., Martinet P. *Adaptive and predictive path tracking control for off-road mobile robots* European journal of control, 13(4):419-439, 2007.

[6] Lenain R., Thuilot B., Cariou C., Martinet P. *High accuracy path tracking for vehicles in presence of sliding. Application to farm vehicle automatic guidance for agricultural tasks* Autonomous robots, 21(1):79-97, 2006.

[7] Montes N., Mora M., Tornero J. *Trajectory generation based on rational Bezier curves as clothoids* IEEE Intelligent Vehicles Symposium, Istanbul, Turkey, june 13-15 2007.

[8] Oksanen T. *Path planning algorithms for agricultural field machines* Helsinki university of technology, research reports No 31, 2007.

[9] Pedersen S.M., Fountas S., Have H., Blackmore B.S. *Agricultural robots - system analysis and economic feasibility* Precision Agriculture, 7(4):295-308, 2006.

[10] Richalet J. *Industrial applications of model based predictive control* Automatica, 29:1251-1574, 1993.

[11] Scheuer A., Laugier C. *Planning sub-optimal and continuous-curvature paths for car-like robots* IEEE/RSJ Int. conf. on intelligent robots and systems, Victoria, Canada, October 12-16, 1998.

[12] Vougioukas S., Blackmore S., Nielsen J., Fountas S. *A two-stage optimal motion planner for autonomous agricultural vehicles*. Precision Agriculture, 7:361-377, 2006.

[13] Walton D.J. *Spiral spline curves for highway design*. Microcomputers in civil engineering 4:99-106, 1989.

[14] Wang D., Low C. B. *Modeling skidding and slipping in wheeled mobile robots: control design perspective*. In Proc. of the IEEE int. conf. on Intelligent Robots and Systems, Beijing, China, Oct 2006.

[15] Zhu Z., Chen J., Yoshida T., Torisu R., Song Z., Mao E. *Path tracking control of autonomous agricultural mobile robots*. Journal of Zhejang University Science A 8(10):1596-1603, 2007.